Google Earth Engine for Assessing Land Use and Land Cover Change in Banyuwangi Regency

Abdul Holik[1][a], Zulis Erwanto[2][b] and Siska Aprilia Hardiyanti[2][c]

[1]Department of Agribusiness, Politeknik Negeri Banyuwangi, Jl. Raya Jember Km 13 Kabat, Banyuwangi, Indonesia
[2]Department of Civil Engineering, Politeknik Negeri Banyuwangi, Jl. Raya Jember Km 13 Kabat, Banyuwangi, Indonesia

Keywords: GEE, Land Use Land Cover, Remote Sensing, Supervised Classification, Banyuwangi.

Abstract: Land use and land cover (LULC) change needs regularly monitor because it causes a multiplayer effect. This study examines the LULC in Banyuwangi regency between 2013 using Landsat-8 and 2021 using Sentinel-2 satellite images data. All processing data used Google Earth Engine (GEE) with supervised classification, classified eight LULC characteristics. The results show that GEE can quickly process image data from the acquisition process, cloud removal, classification to accuracy tests. LULC significant changes in paddy fields (-3.76%) and forests (+3.08%), moderate changes in plantations (+0.44 %), water bodies (-0.39%), built-up (+0.34%), and bare soil (+0.27%), while minor changes occur in field (-0.01%) and shrubs (+0.26%). Even though forest land is increasing, the loss of paddy fields must be a serious concern to maintain the stability of rice stocks.

1 INTRODUCTION

Remote sensing is a popular tool for mapping and monitoring land use/land cover change. It is currently the most reliable tool for monitoring various spectrally sensitive changes of the earth (Alam, Bhat, & Maheen, 2020). Several satellite images like Landsat and Sentinel with band-combination are widely used to detect the changes on a large scale.

Google earth engine (GEE) is a cloud-based platform for geospatial data analysis, especially raster data. GEE provides powerful computing capabilities and provides many remote sensing data and various auxiliary datasets (Qu, Chen, Li, Zhi, & Wang, 2021). GEE can be accessed via an application programming interface (API) over the web-based Internet. Users can prototype, visualize results quickly (Gorelick et al., 2017), and also analyze big geospatial data in a sophisticated way without requiring access to supercomputers or special coding skills (Tamiminia et al., 2020). In addition, (Zurqani, Post, Mikhailova, Schlautman, & Sharp, 2018) demonstrates the advantages of using GEE and the public archive

database on its platform to track and monitor changes in LULC over time.

The impacts caused by land cover changes are a reduction of agricultural land (Wijaya & Susetyo, 2017), implications for groundwater quality (He, Li, Wu, & Elumalai, 2019), sooner and later, the land is converted into wasteland (Ramanamurthy & Victorbabu, 2021). Monitoring of LULC to map needs regular updates. It requires high spatial resolution time-series data to understand better LULC dynamics and their impact on biomass (Jr et al., 2020).

Banyuwangi Regency is the largest regency and the most significant contributor to staple foods in East Java. In the last ten years, Banyuwangi has experienced rapid development (international airport, mining, railway factory, sugar industry factory, building of five-star hotels and villas), so that land use and land cover (LULC) change is inevitable. Rural areas are experiencing profound social-economic transitions driven by industrialization and urbanization (Zhu et al., 2021) as well as Banyuwangi. Practically, land cover change is expected in the developing regions and part of the

[a] https://orcid.org/0000-0001-9987-1161
[b] https://orcid.org/0000-0001-7938-9116
[c] https://orcid.org/0000-0001-6003-6791

regional development indicators. Nevertheless, this certainly impacts the carrying capacity of the environment, especially in the agricultural sector. The monitoring results are expected to be useful for policymakers in Banyuwangi, especially to maintain food stocks in a stable condition.

2 STUDY AREA

The study area covers about 3,600 square kilometres with a coastline of about 175.8 km, including all urban agglomeration which is located between the latitude of 7°43' − 8°46' and longitude of 113°53' − 114°38'. The east, Banyuwangi is bordered by the Bali strait and the west by Ijen mountain, which is 3,200 m high. While the south is bordered directly by the Indian Ocean. The total population of Banyuwangi regency increased from 1,559,088 in 2010 to 1,754,719 inhabitants in 2020 (BPS Badan Pusat Statistik, 2020).

Topographically, the study area can be divided into three distinct regions: the mountainous area located to the west and northwest (Figure 1), north and south dominated by dense forests, and settlements are primarily in flat areas that tend to be close to coastal areas and lowland areas. The average slope level in the western and northern regions is 40°, with a higher average rainfall when compared to other parts of the region.
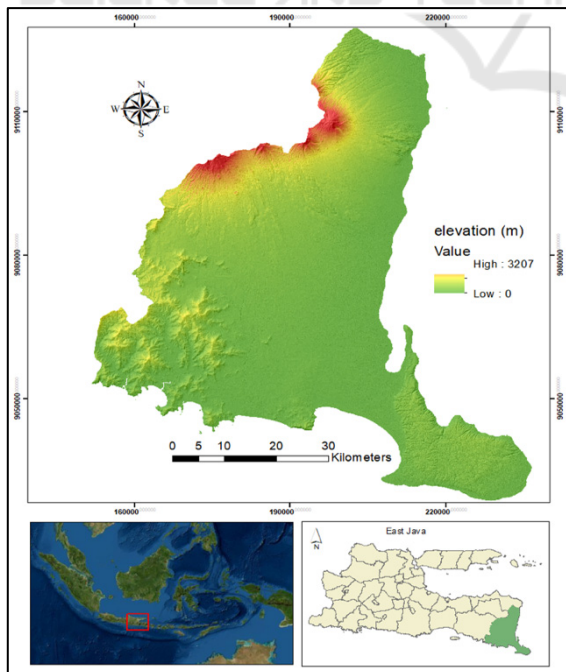

Figure 1: The topographic of Banyuwangi.

Lowlands stretch from south to north. Wherein many rivers always flow in throughout the year. In Banyuwangi, there are 35 watersheds, so that besides being able to irrigate an extensive view of the rice fields as well positive effect on the level of soil fertility. The mountainous region is a plantation product-producing area. Lowland produces primary agricultural products, and areas around the beach line produce various marine biota.

3 METHODS OF DATA ACQUISITION AND ANALYSIS

Landsat images and Sentinel images were collected from the official webpage of the Google Earth Engine (GEE). LULC change monitoring requires data for two different periods. Remote sensing approaches typically use two or more date satellite imagery to measure land use and land cover changes in any area (Alam et al., 2020). In this study, collecting data was in 2013 for Landsat-8 and 2021 for sentinel-2 images. The spatial resolution of the image is 30*30 m to 10*10 m pixel size. The images were georeferenced and projected as the Universal Transverse Mercator (UTM) within Zone 50 S. Details of the satellite data used in this study are presented in Table 1.

Table 1: Characteristic of the datasets.

Data	Spatial resolution	Time acquisition	GEE Image Collection ID
Landsat-8	30 m	2013	LANDSAT/LC08/C01/T1_TOA
Sentinel-2	10 m	2021	COPERNICUS/S2_SR

In this analysis, LULC classification was implemented based on eight classes, and a brief description of major LULC classes is provided in Table 2. This classification is based on the Indonesian National Standard (SNI) 7645:2010. This standard refers to land cover classification united nation – food and agriculture organization LCCS-UNFAO and ISO 19144-1 geographic information system- part 1: classification system structure and developed with phenomena that exist in Indonesia.

Table 2: LULC classification scheme.

LULC type	Description	value
paddy field	the agricultural area that is inundated with water either with irrigation technology, rainfed, low tide, or tidal, which is characterized by a bund pattern, by planting short-lived food crops (paddy)	1
field	an area used for agricultural activities with seasonal crops on dry land	2
plantation	land used for agricultural activities without changing crops for two years	3
shrubs	the dry land area has been overgrown with various heterogeneous and homogeneous natural vegetation; the density level is rare to dense. The area is dominated by low vegetation (natural). Bushes in Indonesia are usually former forest areas and usually do not show any traces or build-up spots anymore	4
forests	forests that grow and develop in dryland habitats which can be lowland forests, hills, mountains, or highland tropical forests	5
built-up area	areas where the natural or semi-natural land cover has been substituted with an artificial land cover, which is usually impermeable and relatively permanent	6
water bodies	all aquatic features, including seas, reservoirs, coral reefs, and seagrass beds	7
bare soil	land without cover, whether natural, semi-natural, or artificial. according to characteristics	8

4 RESULT AND DISCUSSION

4.1 Region of Interest

The first thing that must be done in the classification process is to make a boundary of the study area. This is intended so that the classification process can be carried out correctly without and not going out of the predetermined limits. ROI can be created by uploading a shapefile file and saving it to a GEE's

database. Then during the classification process, this ROI can be recalled and used as a geometry variable.

The script used to call the uploaded data is as follows:

```
var shp =
    ee.FeatureCollection('users/abdu
    lholik/adm_bwi')
Map.addLayer(shp)
```

shp is the variable name, while the script in brackets is a link to the storage location. ROI can be shown by the following Figure 2.
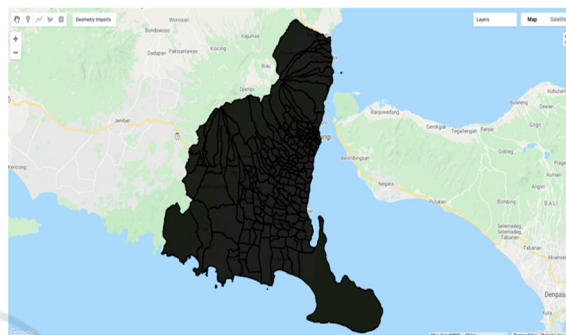

Figure 2: Region of Interest (ROI).

4.2 Image Acquisition

The image acquisition process can be quickly done by looking at the Earth Engine Data Catalog script (https://developers.google.com). It depends on the type of satellite used. Different satellite, then the code name will also be different. The acquired image data can be directly adjusted to the time and condition of the cloud cover, where cloud cover can be cleared all at once.

The script used for Landsat-8 in this process is as follows:

```
var maskL8  = function(image) {
var qa      = image.select('BQA');
var mask    =   qa.bitwiseAnd(1   <<
            4).eq(0);
return image.updateMask(mask);}

var composite =
            ee.ImageCollection('LAND
            SAT/LC08/C01/T1_TOA')
    .filterDate('2013-04-
            01','2013-12-31')
    .map(maskL8)
    .median()
    .clip(shp);
```

While script for sentinel-2 is as follows:

```
function maskS2clouds(image) {
var qa    = image.select('QA60');
var cloudBitMask = 1 << 10;
var cirrusBitMask = 1 << 11;
```

```
var mask =
        qa.bitwiseAnd(cloudBitMask
        ).eq(0).and(qa.bitwiseAnd(
        cirrusBitMask).eq(0));retu
        rn
image.updateMask(mask).divide(10000
        );}

var composite =
        ee.ImageCollection('COPERN
        ICUS/S2_SR')
    .filterDate('2021-01-01', '2021-
        06-30')
    .filter(ee.Filter.lt('CLOUDY_PIX
        EL_PERCENTAGE',20))
    .map(maskS2clouds)
    .median()
    .clip(shp);
```

To visualize the image data, the script is written as follows:

```
var RGBTrue =
    composite.select(['B4', 'B3',
    'B2']);

var RGBparam = {min: 0, max: 0.3,};

Map.addLayer(RGBTrue, RGBparam,
    'TRUE');
```

The results are shown in Figure 3. The true colours displayed are the composite colours of band 4, band 3, and band 2 for landsat-8 and band 5, band 4, and band 3 for Sentinel-2.

Figure 3: True Color composite band.

4.3 Training Area

LULC classes are earned by creating a training area. The training area is an area created to represent the value of each class. It is created by adding a geometry variable and filling it with a name and value (according to Table 2) for each training area as Figure 4.
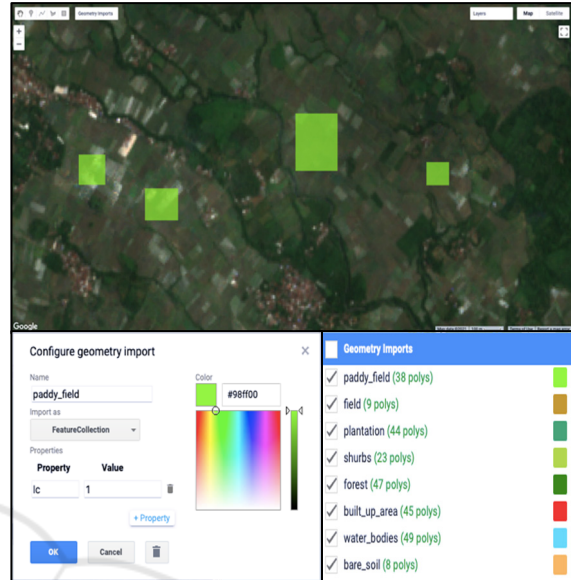

Figure 4: Properties of the training area.

4.4 LULC Classes

After the training area has been created, the next step is to run the classification process through guided classification. In this study, the algorithm used in the classification process uses a random forest. The Random Forest (RF) classification method is used most often and shows minimum and maximum overall accuracy compared to other classifiers (Tamiminia et al., 2020). The classification results are shown by the following Figure 5 and the script used in this step is:

```
var aoi =
    paddy_field.merge(field).merge(plan
    tation).merge(shurbs).merge(forest)
    .merge(built_up_area).merge(water_b
    odies).merge(bare_soil);

var bands =
    ['B1','B2','B3','B4','B5','B6','B7'
    ];

var training =
    composite.select(bands).sampleRegio
    ns({ collection: aoi, properties:
    ['lc'], scale: 30});

var classifier =
    ee.Classifier.smileRandomForest(100
    ).train({features: training,
```

```
classProperty:'lc',inputProperties:
    bands});

var classified =
    composite.select(bands).classify(cl
    assifier);

Map.addLayer(classified,{min: 1, max:
    8,palette:['#98ff00','#c4980e','#46
    a37a','#40ab36','#048711','#ff0000'
    ,'#68d9ff','#ffb868']},'landcover';
```


Figure 5: LULC classification in 2013 and 2021.

4.5 Accuracy Test

The accuracy test is carried out in almost the same way as making a classification, namely making a sample training area. This training area sample is then combined with the classification results for the validation process. The accuracy test script is shown as follows, while the accuracy test matrix is shown in Table 3 and 4.

```
var uji_aoi =
    accuracy_test_paddy_field.merge(acc
    uracy_test_field).merge(accuray_tes
    t_plantation)
```

```
.merge(accuracy_test_shurbs).merge(acc
    uracy_test_forest).merge(accuracy_t
    est_built_up_area).merge(accuracy_t
    est_water_bodies).merge(accuracy_te
    st_bare_soil);

var validasi =
    classified.sampleRegions({collectio
    n: uji_aoi,properties:
    ['lc'],scale: 30,});
print(validasi);

var akurasi =
    validasi.errorMatrix('lc',
    'classification');
print('Confusion matrix', akurasi);
print('Overall accuracy: ',
    akurasi.accuracy());

var class_areas =
    ee.Image.pixelArea().divide(1000*10
    00).addBands(classified)
.reduceRegion({

reducer:
    ee.Reducer.sum().group({groupField:
    1,groupName: 'code',}),geometry:
    shp, maxPixels : 5000000000,scale:
    30,})
.get('groups');

print(class_areas);
```

Table 3: Accuracy of LULC maps obtained from 2013 Landsat-8 satellite data.

Matrix		Sample area test								
		1	2	3	4	5	6	7	8	Total
Class image	1	234	0	0	0	36	1	0	0	271
	2	0	0	0	0	3	0	0	0	3
	3	2	0	33	0	53	0	0	0	88
	4	2	0	1	0	0	0	0	0	3
	5	0	0	2	0	6434	16	0	0	6452
	6	1	0	0	0	4	34	0	0	39
	7	0	0	0	0	0	0	3	0	3
	8	1	0	0	0	1	0	0	0	2
Total		240	0	36	0	6531	51	3	0	6861

Sum of diagonal   = 6738
Total   = 6861
Overall accuracy   = 98.2%

Table 4: Accuracy of LULC maps obtained from 2021 Sentinel-2 satellite data

Matrix		Sample area test								
		1	2	3	4	5	6	7	8	Total
Class image	1	352	0	1	0	2	0	1	0	356
	2	0	0	0	0	0	0	0	0	0
	3	1	0	216	0	0	0	0	0	217
	4	0	0	0	0	0	0	0	0	0
	5	73	12	310	8	35032	1	1	1	35438
	6	0	0	0	0	0	169	0	2	171
	7	0	0	0	0	0	0	47	0	47
	8	0	0	0	0	0	0	0	122	122
Total		426	12	257	8	35034	170	49	125	36351

Sum of diagonal = 35938
Total = 36351
Overall accuracy = 98.8%

4.6 Distribution of LULC Change

The results of the study indicate that all land classes have changed. The most significant changes occurred in paddy fields and forests. Medium changes occur in plantations, water bodies, built-up land, and open land. While minor changes occurred in fields and shrubs, as shown in Table 5.

Paddy fields decreased drastically due to several things: First, changing paddy fields into built-up land. The existence of new settlements caused by the increase in population and the development of several industrial sectors contributed to converting paddy fields into built-up land. Second, the change of paddy fields into forests because farmers convert rice plants into wood plants, namely Sengo *(Albizia Chinensis)*. Third, the conversion of paddy fields into plantations. Many farmers in southern Banyuwangi have turned their fields into dragon fruit plantations (pitaya: *Hylocereus undatus*).

The subsequent reduction in the class category is water bodies and fields. Many water bodies are located around the coast. The decrease in water bodies is caused by many ponds being abandoned because their permits have expired. Then switch functions into mangrove forests, and some of them turn into built-up land. The number of fields is reduced because farmers change their crop commodities into wood plants, so it is included in the forest class.

Table 5: The distribution of land cover classification for each year.

Land use classes	The coverage area for each year					
	2013		2021		change 2013-2021	
	km^2	%	km^2	%	km^2	%
paddy field	514.59	14.24	378.71	10.48	-135.88	-3.759
field	0.59	0.02	0.41	0.01	-0.18	-0.005
plantation	76.48	2.12	92.38	2.56	+15.90	+0.440
shrubs	0.27	0.01	1.36	0.04	+1.09	+0.030
forests	2890.74	79.98	3001.95	83.06	+111.21	+3.077
built-up	101.69	2.81	114.04	3.16	+12.35	+0.342
water bodies	29.8	0.82	15.72	0.43	-14.08	-0.390
bare soil	0.18	0.00	9.75	0.27	+9.57	+0.265
Total	3614.34	100	3614.32	100		

5 CONCLUSIONS

The study results conclude that the GEE Platform can perform high-speed spatial analysis for large areas and large data sets without searching and downloading satellite data for desktop processing. The land class can also be appropriately classified using random forest classification with a very satisfactory level of accuracy.

Significant land changes occur in paddy fields and forests. Even though forest land is increasing, the reduction of lowland rice land must be a severe concern for the government to secure rice as the leading staple food for the people of Banyuwangi. In the future, monitoring of land change must continue to be carried out by assessing the impact of land change on environmental carrying capacity and land criticality in the Banyuwangi Regency.

ACKNOWLEDGEMENTS

REFERENCES

Alam, A., Bhat, M. S., & Maheen, M. (2020). Using Landsat satellite data for assessing the land use and land cover change in Kashmir valley. *GeoJournal*, *85*(6),

1529–1543. https://doi.org/10.1007/s10708-019-10037-x

BPS Badan Pusat Statistik. (2020). Banyuwangi dalam Angka. Retrieved from www.banyuwangikab.bps.go.id

Gorelick, N., Hancher, M., Dixon, M., Ilyushchenko, S., Thau, D., & Moore, R. (2017). Google Earth Engine: Planetary-scale geospatial analysis for everyone. *Remote Sensing of Environment*, *202*, 18–27. https://doi.org/10.1016/j.rse.2017.06.031

He, S., Li, P., Wu, J., & Elumalai, V. (2019). Human and Ecological Risk Assessment : An International Groundwater quality under land use / land cover changes : A temporal study from 2005 to 2015 in. *Human and Ecological Risk Assessment: An International Journal*, *0*(0), 1–27. https://doi.org/10.1080/10807039.2019.1684186

Jr, C. M. S., Shimbo, J. Z., Rosa, M. R., Parente, L. L., Alencar, A. A., Rudor, B. F. T., … Oliveira, S. W. De. (2020). Reconstructing Three Decades of Land Use and Land Cover Changes in Brazilian Biomes with Landsat Archive and Earth Engine. *Remote Sensing*, *12*(2735).

Qu, L., Chen, Z., Li, M., Zhi, J., & Wang, H. (2021). Accuracy Improvements to Pixel-Based and Object-Based LULC Classification with Auxiliary Datasets from Google Earth Engine. *Remote Sensing*, *13*(453).

Ramanamurthy, B. V, & Victorbabu, N. (2021). Land Use Land Cover (LULC) classification with wasteland demarcation using Remote sensing and GIS Techniques. In *IOP Conference Series: Materials Science and Engineering. International Conference on Sustainable Systems and Structures* (p. 012035). IOP Publishing. https://doi.org/10.1088/1757-899X/1025/1/012035

Tamiminia, H., Salehi, B., Mahdianpari, M., Quackenbush, L., Adeli, S., & Brisco, B. (2020). Google Earth Engine for geo-big data applications: A meta-analysis and systematic review. *ISPRS Journal of Photogrammetry and Remote Sensing*, *164*, 152–170. https://doi.org/10.1016/j.isprsjprs.2020.04.001

Wijaya, A., & Susetyo, C. (2017). Analisis Perubahan Penggunaan Lahan di Kota Pekalongan Tahun 2003, 2009, dan 2016. *Jurnal Teknik ITS*, *6*(2), 417–420.

Zhu, C., Lin, Y., Zhang, J., Gan, M., Xu, H., Li, W., … Wang, K. (2021). Exploring the relationship between rural transition and agricultural eco-environment using a coupling analysis : A case study of Zhejiang. *Ecological Indicators*, *127*. https://doi.org/10.1016/j.ecolind.2021.107733

Zurqani, H. A., Post, C. J., Mikhailova, E. A., Schlautman, M. A., & Sharp, J. L. (2018). Geospatial analysis of land use change in the Savannah River Basin using Google Earth Engine. *International Journal of Applied Earth Observation and Geoinformation*, *69*, 175–185. https://doi.org/10.1016/j.jag.2017.12.006